Journal of Sound and Vibration (2000) **231**(4), 1168–1174
doi:10.1006/jsvi.1999.2637, available online at http://www.idealibrary.com on IDEAL®

STRUCTURAL VIBRATION CONTROL USING SHAPE MEMORY ACTUATORS

S.-B. CHOI AND J.-H. HWANG

Smart Structures and Systems Laboratory, Department of Mechanical Engineering, Inha University, Incheon 402-751, *Korea*

(*Received* 1 *June* 1999, *and in final form* 4 *August* 1999)

1. INTRODUCTION

Recently, significant progress has been made in the synthesis of intelligent structures incorporating shape memory alloys (SMA) [1, 2]. These structures are primarily employed to control the static and elastodynamic responses of distributed parameter systems including light space structures. It is well recognized that the SMA actuator produces relatively large control forces, but exhibits slow response time compared to other actuating smart materials such as piezoceramics. Therefore, it is necessary to take into account the dynamic bandwidth of the SMA actuator in the system model in order to accurately evaluate vibration control performance of flexible structures. The goal of this work is to demonstrate the effectiveness of the dynamic bandwidth of the actuator on the vibration suppression capability in a closed-loop control system.

The present work presents a sliding mode control for vibration of a flexible structure with the dynamics of SMA actuator. This is an extension of the previous work [2] in which the actuator dynamic was not considered. The dynamic behavior of the employed SMA actuator is experimentally identified and incorporated with the governing equation of motion of a flexible structure. A sliding mode controller (SMC) for vibration suppression is then designed by treating frequency and damping deviations as uncertain parameters. The controller is experimentally realized and vibration control responses are presented in the time domain.

2. SYSTEM MODELLING

The arrangement of the experimental apparatus for the vibration control is a building-like structure as shown in Figure 1. The purpose is to control the vibration of the above structure excited from the base structure by the shaker. This is accomplished by activating four SMA wire actuators installed with a certain inclined angle. The dynamic model of the proposed system can be formulated through a typical finite element method [1]. Thus, the model can be expressed in

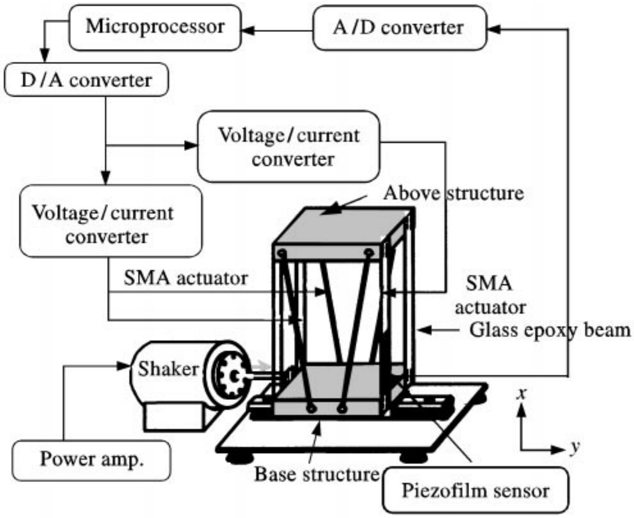

Figure 1. Experimental apparatus for vibration control.

the transformed modal co-ordinate (q) as

$$\ddot{q}_i(t) + 2\zeta_i \omega_i \dot{q}_i(t) + \omega_i^2 q_i(t) = f_a(t), \tag{1}$$

where $f_a(t)$ represents the actuating force, and ζ_i and ω_i denote the ith-mode damping ratio and natural frequency respectively.

The inherent dynamic characteristic of the SMA actuator $f_a(t)$ should first be identified to achieve successful implementation. This is normally accomplished by investigating step-input response of the SMA actuator. Figure 2 presents the measured step response of the employed SMA actuator (Nitinol wire). We see that the actuator dynamic behaves like the first order model. Similar dynamic behavior of the SMA actuator is also observed in reference [1]. Thus, the actuator dynamic can be expressed by

$$\tau \frac{\mathrm{d}f_a(t)}{\mathrm{d}t} + f_a(t) = i(t), \tag{2}$$

where $i(t)$ is the input current and τ is the time constant of the actuator. According to the dynamic model the actuating force produced is linearly dependent on the electrical current driven through the SMA wire. On the other hand, we clearly see from Figure 2 that the time constant at the heating stage (rising) is quite different from the time constant at the cooling stage (falling). This causes the control system to be divided into two parts which is undesirable in the experimental realization. Therefore, in this work we adopt the average value as a nominal time constant. It is remarked that the time constant depends highly on the prestrain that is imposed to the SMA wire. In this work, 5% of the prestrain was imposed. Now, we design a controller on the basis of the system model given by equations (1) and (2).

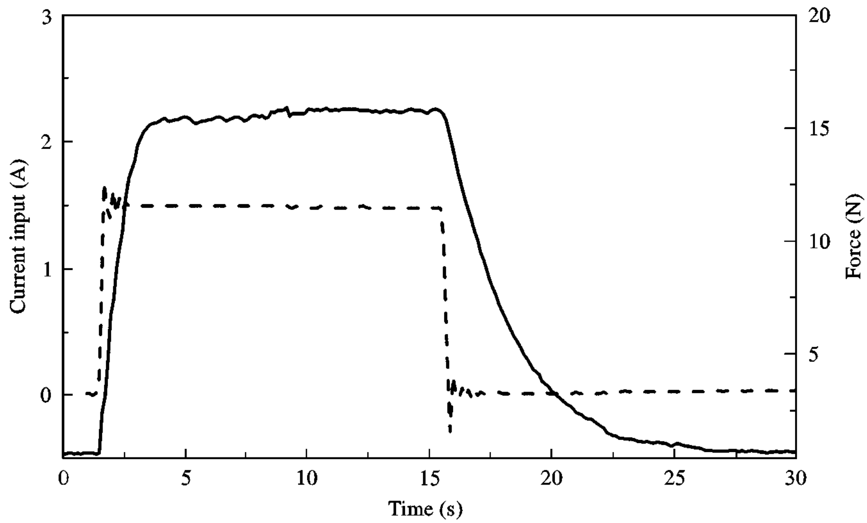

Figure 2. Measured dynamic characteristic of the SMA actuator, —— force; - - - current.

3. SLIDING MODE CONTROLLER

One salient feature of the SMC is the sliding motion of the state on the sliding surface in which the system has invariance property to uncertain parameters. To demonstrate this feature, we impose parameter variations such as natural frequency deviation which can arise due to the imposed additional mass on the above structure. These variations can be expressed as follows [3]:

$$\begin{aligned} \omega_i &= \omega_{0,i} + \delta\omega_i, \quad |\delta\omega_i| \leqslant \beta_i \omega_{0,i}, \\ \zeta_i &= \zeta_{0,i} + \delta\zeta_i, \quad |\delta\zeta_i| \leqslant \gamma_i \zeta_{0,i}, \end{aligned} \tag{3}$$

where $\omega_{0,i}$ and $\zeta_{0,i}$ are the nominal natural frequency and the damping ratio, respectively. The $\delta\omega_i$ and $\delta\zeta_i$ are corresponding possible deviations which are bounded by the weighting factors β_i and γ respectively. By substituting equation (3) into equation (1) yields uncertain control model [3].

As a first step to design the SMC controller, we introduce state errors using the mode shape (Φ) as follows:

$$e_1(t) = y - y_d = \sum_{i=1}^{n} \Phi_i(L) \cdot q_i(t) - y_d,$$

$$e_2(t) = \dot{y} - \dot{y}_d = \sum_{i=1}^{n} \Phi_i(L) \cdot \dot{q}_i(t) - \dot{y}_d,$$

$$e_3(t) = \ddot{y} - \ddot{y}_d = \sum_{i=1}^{n} \Phi_i(L) \cdot \ddot{q}_i(t) - \ddot{y}_d. \tag{4}$$

Here y (refer to Figure 1) is the actual displacement of the above structure to be controlled and y_d is the desired one which is set to be zero in order to suppress the deflection as much and as rapidly as possible. Thus, we determine the following sliding surface using error state:

$$s = \lambda^2 e_1(t) + 2\lambda e_2(t) + e_3(t), \quad \lambda > 0. \tag{5}$$

We now design the following sliding mode controller (input current $i(t)$) which satisfies the SMC $s\dot{s} < 0$ [3]:

$$i(t) = -\left(\frac{1}{P}\right)\left\{\lambda^2 e_2(t) + 2\lambda e_3(t) + \left[\left(r_{2i} + \frac{1}{\tau}\right)\ddot{q}_i(t) + \left(r_{2i-1} + \frac{r_{2i}}{\tau}\right)\dot{q}_i(t) + \left(\frac{r_{2i-1}}{\tau}\right)q_i(t)\right.\right.$$

$$\left.\left. + \left[k_g + \left|z_{2i}\ddot{q}_i(t) + \left(z_{2i-1} + \frac{z_{2i}}{\tau}\right)\dot{q}_i(t) + \left(\frac{z_{2i-1}}{\tau}\right)q_i(t)\right|\right]\operatorname{sgn}(s)\right\}, \tag{6}$$

where

$$r_{2i} = -2\zeta_{0,i}\omega_{0,i}, \quad r_{2i-1} = -\omega_{0,i}^2,$$

$$z_{2i-1} = -(2\omega_{0,i}\beta_i\omega_{0,i} + \beta_i^2\omega_{0,i}^2),$$

$$z_{2i} = -2(\gamma_i\zeta_{0,i}\omega_{0,i} + \beta_i\omega_{0,i}\zeta_{0,i} + \gamma_i\beta_i\zeta_{0,i}\omega_{0,i}). \tag{7}$$

In the above, P is the generalized mass, k_g (>0) is the control gain, and sgn($*$) denotes a signum function. The implementation of the controller given by equation (6) causes chattering in the control history which is an impediment to the SMC. Thus, the sgn($*$) in the controller is replaced by saturation function in the experimental realization. It is clearly recognized that the SMC given by equation (6) is designed by considering both the actuator dynamics and parameter variations. This is the main contribution of the present work compared with the previous work [2]. Control performances due to these characteristics are to be investigated in a subsequent experimental realization.

4. EXPERIMENTAL RESULTS

The employed glass epoxy beam is 350 mm long, 45 mm wide, and 2 mm thick. The diameter of the SMA actuator wire is 0·36 mm and its transformation temperature is 36°C. The phase transformation of the Nitinol wire used in this work is the austenite/martensite. The actuators are installed between the base and the structures above at an angle of 15·0°. In Figure 1, the vibration magnitude of the above structure is measured from the piezofilm sensor bonded on the surface of the beam, and fed back to the microprocessor through the A/D converter which has 12 bits. The controller is implemented using a personal computer (IBM586) with a sampling frequency of 1000 Hz. The first two vibration modes are considered and

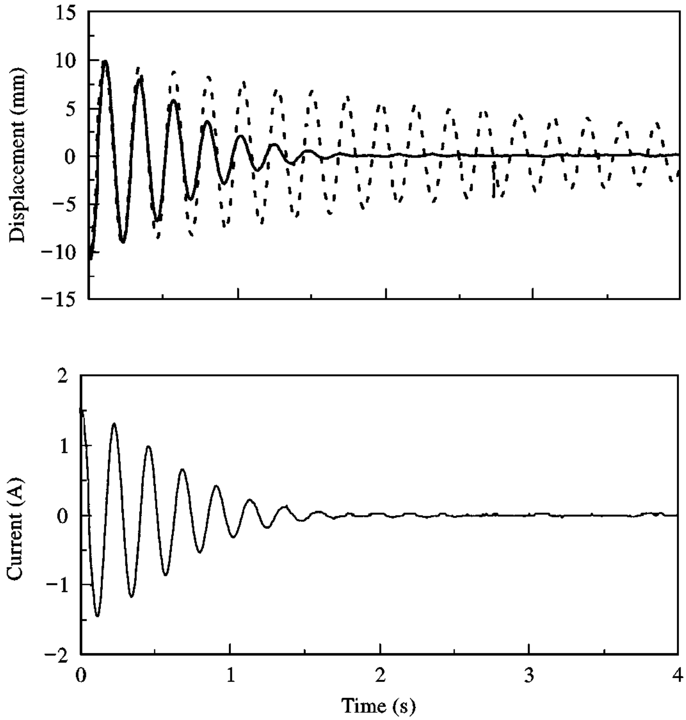

Figure 3. Measured transient-vibration control responses, ---- open-loop; —— closed-loop.

the following control parameters are employed: $\tau = 125$ ms, $k_g = 2{\cdot}5$, $\lambda = 12{\cdot}5$, $\beta_1 = 12\%$, $\beta_2 = 5\%$, $\gamma_1 = 10\%$ and $\gamma_2 = 5\%$.

Figures 3 and 4 present measured transient and forced vibration control responses. The transient vibration response was generated by imposing an initial displacement at the above structure of 10 mm, while the forced vibration response was obtained by vibrating the base structure with the first-mode natural frequency of 4·63 Hz. It is clearly observed that the imposed vibration was favorably suppressed in both cases by employing the proposed controller. In the controller implementation, an additional mass of 0·5 kg was imposed on the above structure to intentionally cause parameter variations such as natural frequency. Therefore, the control results shown in Figures 3 and 4 validate the robustness of the proposed sliding mode controller. It is remarked that the actuating force produced from the SMA actuator does not change sign when the electrical input current is reversed. Thus, the positive sign of the input current shown in Figures 3 and 4 is for the pair of SMA actuators installed in the left side (refer to Figure 1), while the negative sign is for the right side.

Now, in order to investigate the effect of the slow response of the SMA actuator on the vibration control, we vibrate the structure by 15 Hz which is beyond the actuator bandwidth (refer to the time constant of 125 ms). It is noted that the second mode natural frequency of the structural system is 50·0 Hz. Figure 5 presents the measured forced vibration control response with the excitation of

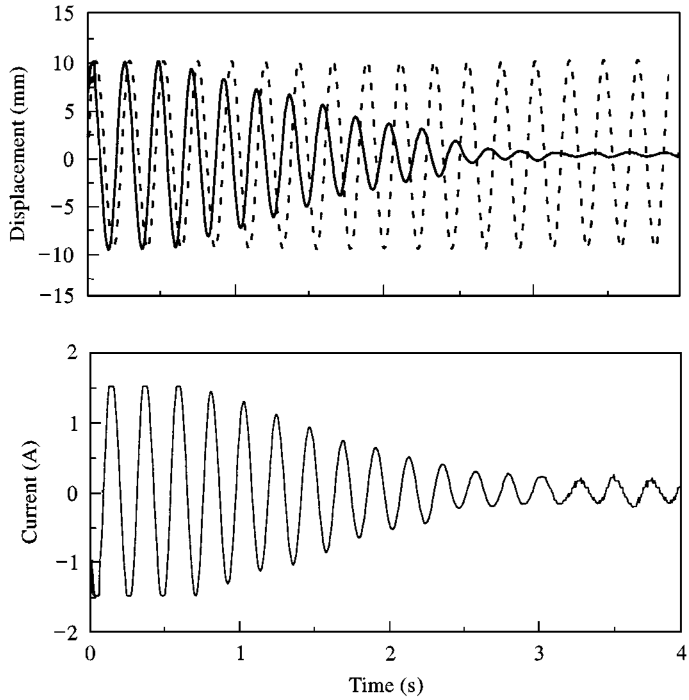

Figure 4. Measured forced-vibration control response, ---- open-loop; —— closed-loop.

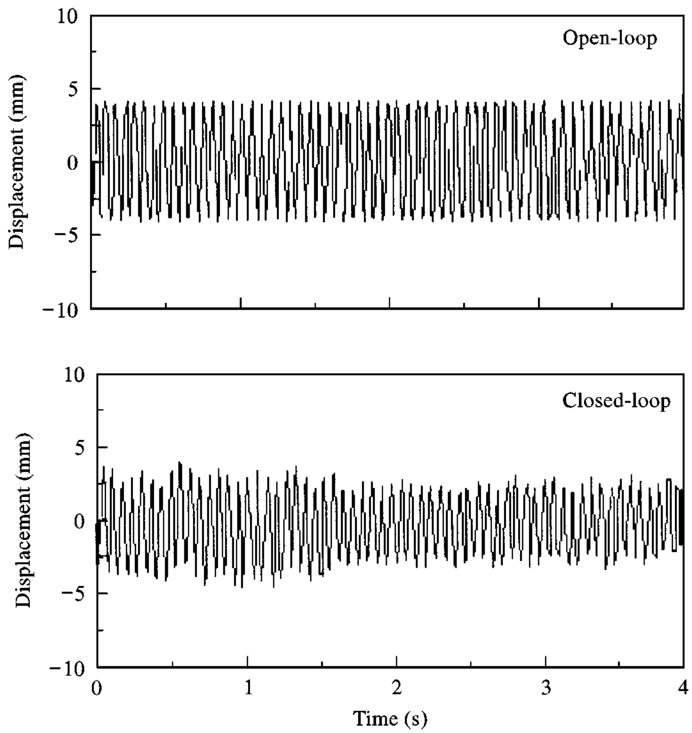

Figure 5. Vibration control limitation due to slow response of the SMA actuator.

15 Hz. It is clearly seen that the imposed vibration is not effectively suppressed. This result is not surprising, but directly indicates the very important fact that the actuator dynamics should be incorporated into the system model, especially when we want to accurately evaluate vibration control performance of flexible structures associated with high-frequency vibration modes.

5. CONCLUSION

An active vibration control of a flexible structure has been undertaken by employing the SMA exhibiting relatively slow dynamic characteristics. It has been shown through experimental realization of a SMC that a successful vibration suppression was achieved when the structural system was excited by the frequency below the actuator bandwidth. However, vibration control performance was not favourable when excited by the frequencies above the actuator bandwidth. This result directly suggests that the dynamics of the SMA which produces relatively slow response characteristics should be identified and incorporated with the system model in order to evaluate accurate vibration control performance.

REFERENCES

1. A. Baz, K. Inman and J. McCoy 1990 *Journal of Sound and Vibration* **140**, 437. Active vibration control of flexible beam using shape memory actuators.
2. S. B. Choi and C. C. Cheong 1996 *Journal of Guidance and Dynamics* **19**, 1178. Vibration control of a flexible beam using shape memory alloy actuators.
3. S. B. Choi, C. C. Cheong and H. C. Shin 1995 *Journal of Sound and Vibration* **179**, 737. Sliding mode control of vibration in a single link flexible arm with parameter variations.